The Single Chlorophyll *a* Molecule in the Cytochrome b_6f Complex: Unusual Optical Properties Protect the Complex against Singlet Oxygen

Naranbaatar Dashdorj,* Huamin Zhang,† Hanyoup Kim,* Jiusheng Yan,† William A. Cramer,† and Sergei Savikhin*

*Department of Physics and †Department of Biological Sciences, Purdue University, West Lafayette, Indiana 47907

ABSTRACT The cytochrome b_6f complex of oxygenic photosynthesis mediates electron transfer between the reaction centers of photosystems I and II and facilitates coupled proton translocation across the membrane. High-resolution x-ray crystallographic structures (Kurisu et al., 2003; Stroebel et al., 2003) of the cytochrome b_6f complex unambiguously show that a Chl *a* molecule is an intrinsic component of the cytochrome b_6f complex. Although the functional role of this Chl *a* is presently unclear (Kühlbrandt, 2003), an excited Chl *a* molecule is known to produce toxic singlet oxygen as the result of energy transfer from the excited triplet state of the Chl *a* to oxygen molecules. To prevent singlet oxygen formation in light-harvesting complexes, a carotenoid is typically positioned within ~4 Å of the Chl *a* molecule, effectively quenching the triplet excited state of the Chl *a*. However, in the cytochrome b_6f complex, the β-carotene is too far (≥14 Å) from the Chl *a* for effective quenching of the Chl *a* triplet excited state. In this study, we propose that in this complex, the protection is at least partly realized through special arrangement of the local protein structure, which shortens the singlet excited state lifetime of the Chl *a* by a factor of 20–25 and thus significantly reduces the formation of the Chl *a* triplet state. Based on optical ultrafast absorption difference experiments and structure-based calculations, it is proposed that the Chl *a* singlet excited state lifetime is shortened due to electron exchange transfer with the nearby tyrosine residue. To our knowledge, this kind of protection mechanism against singlet oxygen has not yet been reported for any other chlorophyll-containing protein complex. It is also reported that the Chl *a* molecule in the cytochrome b_6f complex does not change orientation in its excited state.

INTRODUCTION

In oxygenic photosynthesis, the integral membrane cytochrome b_6f redox complex connects the reaction centers of photosystems I and II electronically by oxidizing lipophilic plastoquinol and reducing plastocyanin or cytochrome c_6 as discussed, for example, in Cramer et al. (1996). This electron transfer process is coupled to proton translocation across the membrane that generates a transmembrane electrochemical proton gradient used to synthesize adenosine triphosphate. The cytochrome b_6f complex accepts one electron from doubly reduced dihydroplastoquinone through a high-potential electron transfer chain that consists of the Rieske iron-sulfur protein and cytochrome *f*. This results in the release of two protons to the aqueous lumenal phase of the membrane (Fig. 1 *A*). The second electron from dihydroplastoquinone is transferred across the complex through two *b* hemes (Berry et al., 2000; Kramer and Crofts, 1993; Meinhardt and Crofts, 1983; Rich, 1984; Trumpower, 1990) or as anionic plastosemiquinone (Girvin and Cramer, 1984; Joliot and Joliot, 1994), and the resulting proton uptake from the stromal side generates an electrochemical proton gradient across the membrane (Fig. 1 *A*).

According to the x-ray structure analysis (Kurisu et al., 2003; Stroebel et al., 2003), the monomeric unit of the 217 kD dimeric cytochrome b_6f complex consists of four large subunits, cytochrome *f*, cytochrome b_6, the Rieske iron-sulfur protein, and subunit IV, and four small subunits, PetG, PetL, PetM, and PetN. In addition, it contains eight natural prosthetic groups: four hemes, one [2Fe-2S] cluster, one Chl *a*, one β-carotene, and one plastoquinone (Fig. 1 *B*). The presence of the Chl *a* in the crystallographic structures unequivocally confirms the earlier findings through biochemical analysis (Bald et al., 1992; Huang et al., 1994; Pierre et al., 1995) of a chlorophyll molecule as an intrinsic component of the cytochrome b_6f complex and raises intriguing questions about the role of the Chl *a*. The function of the cytochrome b_6f complex does not require light harvesting, and the Chl *a* molecule is not part of the electron transfer chain, which are the usual functions of the chlorophyll molecule in photosynthetic complexes. Moreover, the functionally similar cytochrome bc_1 complex of the respiratory chain does not contain a Chl *a* molecule (Hunte et al., 2000; Iwata et al., 1998; Xia et al., 1997; Zhang et al., 1998).

Regardless of the role of the Chl *a* in the cytochrome b_6f complex, the introduction of a chlorophyll molecule into the protein structure may pose a serious threat to the stability of

Submitted December 24, 2004, and accepted for publication March 16, 2005.

Address reprint requests to Sergei Savikhin, Tel.: 765 494 3017; Fax: 765-494-0706; E-mail: sergei@physics.purdue.edu.

Abbreviations used: Chl *a*, chlorophyll *a*; DAS, decay-associated spectra; fwhm, full width at half-maximum; ML, *Mastigocladus laminosus*; MLb_6f, cytochrome b_6f complex from ML; MLb_6f-crystal, dissolved x-ray diffraction quality crystals of the cytochrome b_6f complex from ML; SC, *Synechococcus* PCC 7002; SCb_6f, cytochrome b_6f complex from SC; Sp, spinach chloroplast; Spb_6f, cytochrome b_6f complex from Sp; carotenoid, Car.

0006-3495/05/06/4178/10 $2.00

doi: 10.1529/biophysj.104.058693

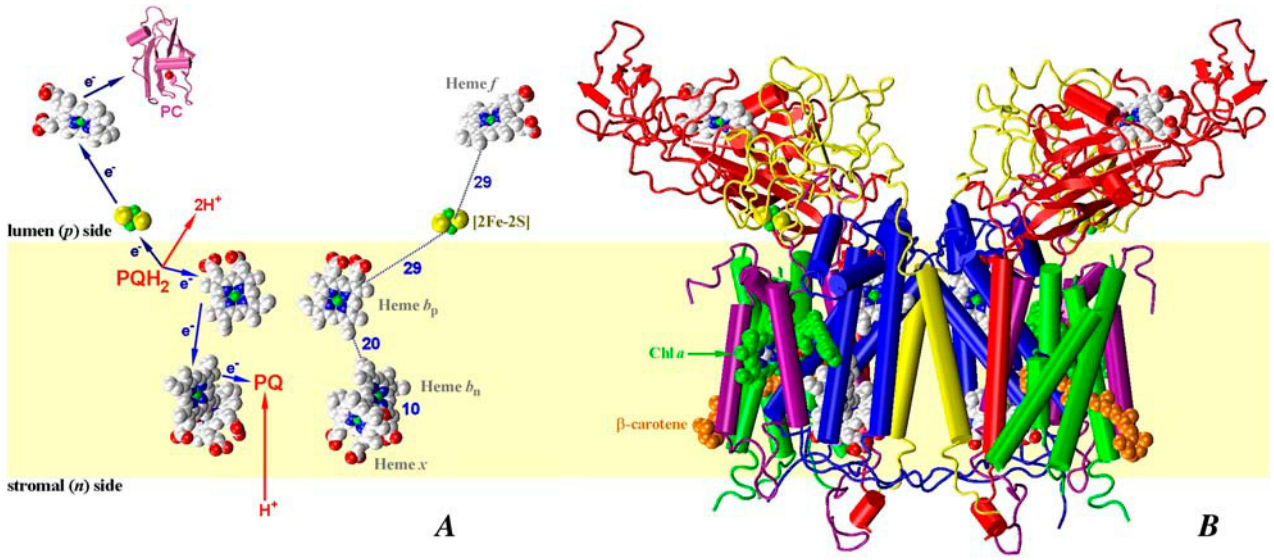

FIGURE 1 Eight subunit dimeric cytochrome b_6f complex of ML. (*A*) Electron and proton transfer pathway through the cytochrome b_6f complex, showing electron and proton transfer stoichiometry for one turnover of the complex and center-to-center distances between redox cofactors. (*B*) Side view showing bound cofactors and protein subunits. The color code is as follows: cytochrome b_6 (*blue*); subunit IV (*purple*); cytochrome *f* (*red*); Rieske iron-sulfur protein (*yellow*); PetG, -L, -M, and -N (*green*); and hydrophobic part of the membrane bilayer (*yellow band*).

the complex. The triplet excited state of the Chl *a* molecule (^{3}Chl*) is known to transfer its energy with almost 100% efficiency to oxygen, generating singlet oxygen (O_2*) that is extremely toxic to the pigment-protein complex (Krinsky, 1979). Under illumination, the triplet excited state of monomeric Chl *a* in solution forms with high quantum yield (~64%) through intersystem crossing from the Chl *a* singlet excited state (Chl*;Bowers and Porter, 1967). To prevent singlet oxygen formation in chlorophyll-containing proteins, Car is typically positioned close (~4 Å) to the Chl *a* molecule, effectively quenching the triplet excited state of the Chl *a* due to rapid triplet-triplet energy transfer to Car (Foote, 1976; Siefermann-Harms, 1987). It was widely expected that a similar protection mechanism would exist in the cytochrome b_6f complex. In fact, along with the Chl *a* molecule, a β-carotene was found to be stoichiometrically bound in the cytochrome b_6f complex (Zhang et al., 1999). It was also reported that, qualitatively, the rate of photodegradation of the Chl *a* depended inversely on the carotene concentration (Zhang et al., 1999).

However, the structures of the cytochrome b_6f complex (Kurisu et al., 2003; Stroebel et al., 2003) show that the β-carotene is too far removed ($\geq$14 Å) from the Chl *a* for effective direct quenching of the Chl *a* triplet excited state. Triplet-triplet energy transfer from ^{3}Chl* to Car occurs via the Dexter type exchange mechanism and requires the interacting cofactors to form a collision complex, restricting triplet-triplet energy transfer to rather short distances (Renger, 1992; van Grondelle et al., 1994).

In this study, it is reported that effective protection against singlet oxygen formation in the cytochrome b_6f complex is, at least in part, realized through an alternative mechanism that has not been reported previously. Optical ultrafast pump-probe experiments reveal that the Chl *a* in enzymatically active ultrapure cytochrome b_6f complex exhibits an unusually short excited state lifetime of ~200 ps that is a factor of ~25 times shorter than the excited state lifetime of monomeric Chl *a* in solution. This result is in good agreement with the data obtained by Peterman et al. (1998) for enzymatically inactive complexes using fluorescence techniques. We found that, due to the short lifetime of the Chl singlet excited state, the formation of the ^{3}Chl* state is dramatically reduced, which would result in a decrease of the consequent production of O_2* in the complex. It was inferred that excitation-induced electron transfer interaction with nearby aromatic amino acid residue(s) is the most likely explanation for the observed effect. Based on the new structure data, it is proposed that the local structure around the Chl *a* facilitates rapid quenching of the Chl* state and thereby minimizes the formation of singlet oxygen.

EXPERIMENTAL PROCEDURES

Sample preparation

Purification and crystallization of the cytochrome b_6f complex is described in detail elsewhere (Zhang et al., 2003; Zhang and Cramer, 2004).

Cytochrome b_6f complexes were purified from the thermophilic cyanobacterium ML, Sp, and the cyanobacterium *Synechococcus* PCC 7002. Complexes from ML and Sp were in enzymatically active dimeric form and contained ~1.1–1.3 Chl *a* molecules per cytochrome *f*. The latter value was determined from the ratio of the cytochrome *f* absorbance at 556 nm for ML and 554 nm for spinach, calculated on the basis of the ascorbate-reduced minus ferricyanide-oxidized difference spectra, and baseline corrected absorption of the Q_y band of Chl *a* using extinction coefficients of 26 $mM^{-1}cm^{-1}$ for cytochrome *f* (Metzger et al., 1997) and 75 $mM^{-1}cm^{-1}$

for Chl *a* (Dawson et al., 1986). The purified preparation of the cytochrome b_6f complex from *Synechococcus* PCC 7002 contained Chl *a* at a 1.0:1 stoichiometry per cytochrome *f* and was in enzymatically inactive monomeric form.

The stoichiometry of Chl *a* relative to cytochrome *f* was critical for unambiguous interpretation of the experimental results. To ensure highest sample purity, ~60 x-ray diffraction quality single crystals of the MLb_6f were dissolved in a buffer containing 30 mM Tris·HCl (pH 7.5), 50 mM NaCl, and 0.05% undecyl-β-D-maltoside. The crystals had a stoichiometry of Chl *a* 1.0:1 relative to cytochrome *f* and contained complexes in a functionally active form exhibiting a rate of 200–300 electrons per cytochrome *f* per second for electron transfer from decyl-plastoquinol to plastocyanin-ferricyanide (Zhang et al., 2003).

Spectroscopic measurements

Steady-state absorption spectra were measured using a PerkinElmer (Wellesley, MA) Lambda 3B spectrometer.

For time-resolved experiments, excitation pulses (660 nm, ~100 fs fwhm) were generated using a self-mode-locked Ti:sapphire laser, regenerative amplifier, optical parametric amplifier, and frequency doubler as described earlier (Savikhin et al., 1999). Transient sample absorption was probed with broadband femtosecond light continuum pulses generated in a sapphire plate; cross correlations between the pump and probe pulses were typically 100–200 fs fwhm. Continuum probe pulses were split into signal and reference beams, dispersed in an Oriel (Stratford, CT) MS257 imaging monochromator operated at ~3 nm bandpass, and directed onto separate Hamamatsu (Bridgewater, NJ) S3071 Si pin photodiodes. The probe, reference, and pump pulse energies were measured in Stanford Research Systems (Sunnyvale, CA) SR250 boxcar integrators, digitized, and processed in a computer. Noise performance was near shot noise limited; the root mean square noise in ΔA was $\sim 3 \times 10^{-5}$ for 1 s accumulation time. Samples were housed in a cell with a 1 mm path length and exhibited ~0.1 absorbance at an excitation wavelength of 660 nm; the excitation density was ~100 μJ/cm^2 (~100 nJ/pulse, ~300 μm spot size). This yielded an excitation rate of 1 out of every ~10 Chls per excitation pulse. The measured kinetic profiles were independent of the excitation intensities.

The pump and probe polarizations were rapidly alternated between parallel and perpendicular using a Meadowlark Optics LRC-200-IR1 liquid crystal variable retarder (Longmont, CO); the time-resolved transient absorption difference at the magic angle (ΔA) and the optical anisotropy (r) were then computed from the respective absorbance difference signals ($\Delta A_\parallel$ and $\Delta A_\perp$) using the following formulae:

$$\Delta A(t) = \Delta A_\parallel(t) + 2\Delta A_\perp(t)$$
$$r(t) = \frac{\Delta A_\parallel(t) - \Delta A_\perp(t)}{\Delta A_\parallel(t) + 2\Delta A_\perp(t)}. \quad (1)$$

Irreversible degradation of the Chl *a* in the cytochrome b_6f complex and monomeric Chl *a* dissolved in organic solvents in an air-saturated environment was induced by controlled irradiation with light generated using a home-built tunable dye laser. Photodegradation was assayed by the integrated area under the Chl *a* Q_y absorbance band (640–700 nm) as a function of irradiation time. Molecular Chl *a* was purchased from Sigma-Aldrich (St. Louis, MO) and dissolved in organic solvents. The monomeric state of Chl *a* and the absence of aggregation in solutions was confirmed by characteristic absorption spectra (Hoff and Amesz, 1990; Vladkova, 2000). The sample was housed in a cell with a 1 mm path length and held at 4°C. The sample absorbance was kept below 0.1 to ensure uniform excitation throughout the sample. The output of the dye laser was expanded to ensure uniform sample irradiation. Chl *a* dissolved in ethanol, methanol, acetone, or Triton X-100 detergent was illuminated at 664.5 nm with an irradiant power density of 0.7 W/cm^2. Samples of cytochrome b_6f complex were photodegraded using 670 nm laser beam with irradiance of 4.5 W/cm^2. Based on the measured absorbance and irradiance intensity values, the average excitation rate (s^{-1}) of a Chl *a* molecule was calculated, and the photodegradation kinetics were normalized to 10 excitations per second, which corresponds approximately to the excitation rate of a single Chl *a* molecule under full sunlight.

RESULTS

Chl *a* is an intrinsic component of the cytochrome b_6f complex

According to the x-ray crystallographic structures (Kurisu et al., 2003; Stroebel et al., 2003) of the cytochrome b_6f complex, the monomeric Chl *a* molecule is bound between helices F and G of subunit IV, with the phytyl tail threading through the portal connecting the electropositive (*p*) quinone-binding niche, and the central quinone-exchange cavity (Fig. 1 *B*). The chlorin ring of the Chl *a* is parallel to the plane of the heme b_n, which is separated by ~16 Å center-to-center from the Chl *a*, whereas the 9-*cis* β-carotene molecule near the center of the transmembrane region is ~14 Å (the closest distance) from the Chl *a* (Fig. 2, as in Kurisu et al., 2003; Stroebel et al., 2003).

Absorbance spectra of the cytochrome b_6f complexes

The absorbance spectra of the cytochrome b_6f complexes are shown in Fig. 3. The most intense peak in the absorbance spectra is centered around 417 nm and is due to the Soret bands of the hemes, whereas the shoulder at ~435 nm arises from the Soret band of the Chl *a*. The shoulders around 455 nm and 485 nm are due to the absorbance of the 9-*cis* β-carotene. The α-band peaks of the hemes in the spectral interval of 515–580 nm are not pronounced in these absorbance spectra since the hemes are oxidized under aerobic conditions.

The differences in the absorbance spectra observed in the spectral region of 630–700 nm reflect slightly different

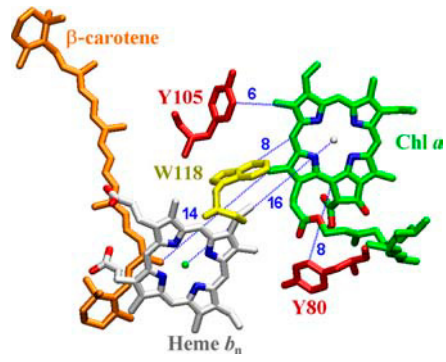

FIGURE 2 Nanospace of the monomeric Chl *a* molecule in the cytochrome b_6f complex (Kurisu et al., 2003). Edge-to-edge distances to the three closest Tyr and Trp residues are specified in the context of electron transfer (Hanson, 1990; Moser et al., 1995; Page et al., 1999).

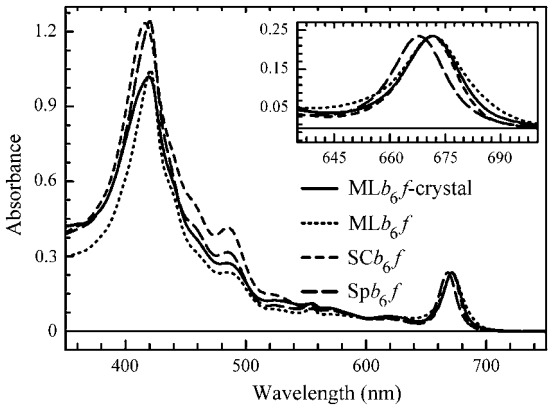

FIGURE 3 Absorbance spectra of the MLb_6f, SCb_6f, Spb_6f, and MLb_6f-crystal.

optical properties of the Chl *a* molecule in these samples and may indicate that the local protein structures around the Chl *a* vary for complexes isolated from different species (Fig. 3, *inset*). The Chl *a* Q_y bands in the MLb_6f-crystal and SCb_6f have maxima at 671.5 nm and fwhm of 17 nm, whereas in MLb_6f and Spb_6f, the Q_y bands of Chl *a* are centered at 671.5 nm and 668 nm and have fwhm of 20 nm and 17 nm, respectively. The absorbance of the Chl *a* in Spb_6f is similar to that in the b_6f complex of *Chlamydomonas reinhardtii* reported by Pierre et al. (1997). The Q_y absorption band of Chl *a* at room temperature did not depend on the redox state of the cytochrome b_6f complex, as it was not affected by the addition of dithionite, ascorbate, or ferricyanide (data not shown).

Kinetics of the singlet excited state of the monomeric Chl *a* in the cytochrome b_6f complex

The ultrafast kinetics of the singlet excited state of the monomeric Chl *a* in the cytochrome b_6f complexes from the four studied samples were probed by femtosecond time-resolved pump-probe spectroscopy. The samples were excited at 660 nm, and absorbance difference kinetics were recorded at 5 nm intervals at multiple probe wavelengths covering the entire Q_y absorption band of the Chl *a* between 665 nm and 695 nm.

Stoichiometry of Chl *a* in the cytochrome b_6f complex is critical for unambiguous interpretation of the results

Purified preparations of the cytochrome b_6f complexes in active dimeric form usually contain nonspecifically bound Chl *a*. Depending on the preparation, these contaminant Chl *a* molecules may account for 10–30% of the total Chl *a* contents in the cytochrome b_6f complexes. Our optical experiments cannot distinguish the signals arising from the native intrinsic bound Chl *a* from signals that stem from the nonspecifically bound Chl *a* that would obscure interpretation of the data. To ensure highest sample purity and to simplify the data analysis, we performed ultrafast pump-probe experiments on the cytochrome b_6f complex obtained by redissolving 60 diffraction quality single crystals (labeled as MLb_6f-crystal).

Fig. 4 shows the absorption difference kinetics for the MLb_6f complexes purified by conventional means, probed at 680 nm after exciting a sample at 660 nm, and that for the MLb_6f-crystal complexes purified through crystallization. Visual inspection of the two profiles and the exponential fits to the data reveal major differences. The ΔA kinetics of the dissolved single crystals can be described by one major decay component of 194 ps (91.2%) accompanied by a weak 5.5 ns (8.8%) component (the respective amplitudes are given in brackets). The optimized fit of the profile obtained for the MLb_6f complex purified by conventional means requires at least three decay components: 6.5 ps (24.6%), 153 ps (62.4%), and 5.5 ns (13%). The main component in the crystal-purified sample is 194 ps and thus it can be ascribed to the ground state recovery process of the intrinsic Chl *a* in the cytochrome b_6f complexes. The 6.5 ps component is not present in the ΔA signal measured for the MLb_6f-crystal and therefore can be ascribed entirely to the contaminant Chl *a*. The longest component lifetime of 5.5 ns could not be reliably determined due to the limited time window. It was, however, similar to the lifetime of monomeric Chl *a* in solution (Seely and Connolly, 1986), and it is attributed to a small fraction of Chl *a* molecules whose excited state properties were not affected by the environment. We also observed a similar 5.5 ± 3 ns major component under analogous excitation conditions in the pump-probe kinetics

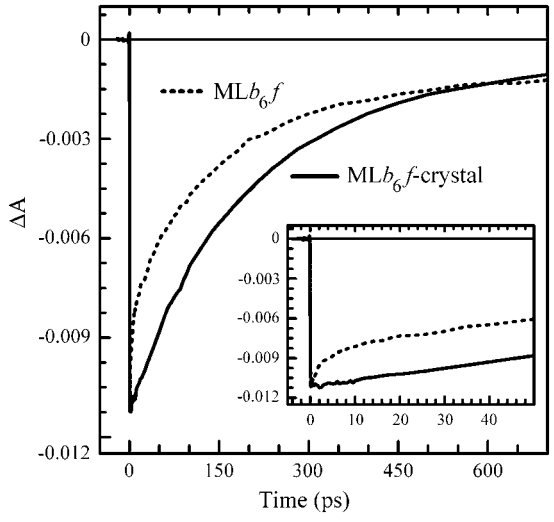

FIGURE 4 Time-resolved transient absorption difference profiles probed at 680 nm after excitation at 660 nm for MLb_6f and MLb_6f-crystal. (*Inset*) The same kinetic profiles at early times.

of the Chl *a* dissolved in organic solvents (data not shown). The main component in the conventionally purified MLb_6f (153 ps) was somewhat shorter than that found in the MLb_6f-crystal complex, indicating that some of the nonspecifically bound Chl *a* have lifetimes shorter than 194 ps and influence the best fit parameters in a model with only three decay components.

The ΔA kinetics for SPb_6f could be described with three components similar to the ones obtained by fitting the data for the MLb_6f complexes, indicating that the dynamics of the Chl *a* excited state in these species are very similar. In contrast, the ΔA profiles for the SCb_6f complexes could be fit with a single decay component with a lifetime of 230 ps, implying that the monomeric inactive complexes contain a significantly smaller pool of nonspecifically bound Chl *a*.

Global analysis of ultrafast time-resolved absorption difference profiles

All time-resolved ΔA profiles for the MLb_6f-crystal complex probed at several wavelengths between 665 nm and 695 nm could be fit globally with four common decay components having lifetimes of 430 fs, 12 ps, 200 ps, and 5.5 ns. The probe-wavelength-dependent amplitudes of these components were assembled into the DAS shown in Fig. 5. The DAS are dominated by the 200 ps component, which corresponds to the monomeric Chl *a* ground state recovery kinetics, as its spectral shape is consistent with the photobleaching spectrum of the monomeric Chl *a*. The amplitudes of the DAS of the 12 ps and 5.5 ns components are small and their spectral shapes are broad. We ascribe these components to a small heterogeneous pool of nonspecifically bound Chl *a*. Similar DAS components with larger amplitudes were observed in the absorption difference profile of MLb_6f complex, which had a higher concentration of nonspecifically bound Chl. The global analysis also yielded a 430 fs component, which can be, at least in part, attributed to vibrational relaxation of the Chl* that is known to occur on this timescale (Savikhin and Struve, 1994). The global analysis of the transient time-resolved absorption difference profiles for SCb_6f and Spb_6f yielded similar decay times.

Ultrafast time-resolved anisotropy

The Chl *a* is embedded deeply in the cytochrome b_6f structure. Stroebel et al. (2003) suggested that this arrangement could facilitate interaction with other components of the photosynthetic apparatus. The plane of the Chl *a* may be, for example, ''twisted'' in response to absorption of light and cause structural response of the protein that could propagate through the cytochrome b_6f and signal proteins, e.g., LHC kinase, on the stromal side of the membrane. To test that hypothesis, we monitored the orientation of the Chl *a* in excited state by measuring the anisotropy $r(t)$ of the ΔA signal probed by polarized light at wavelengths ranging from 665 nm to 695 nm after excitation of the complex at 660 nm. The anisotropy dynamics showed negligible dependence on the probe wavelength, and only one trace measured at 680 nm for the MLb_6f-crystal complex is shown in Fig. 6. The anisotropy is 0.37, which is close to the theoretical maximum of 0.4 for a completely rigid molecule with parallel absorption and emission transition dipole moments. It is almost constant during the lifetime of the Chl *a* excited state indicating that, during this time (~200 ps), Chl *a* excitation does not lead to detectable reorientation of the molecule.

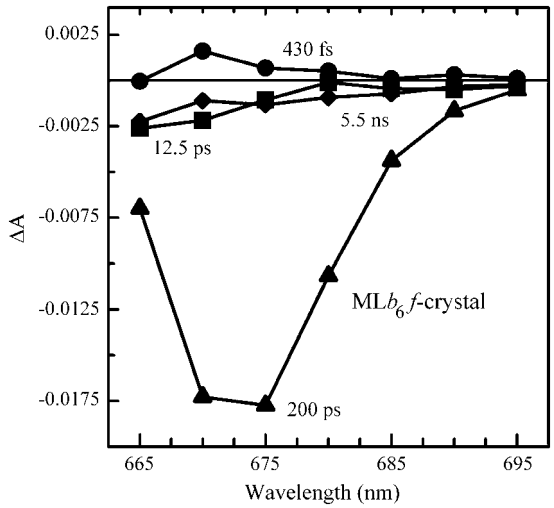

FIGURE 5 DAS obtained by global analysis of ΔA profiles for the MLb_6f-crystal.

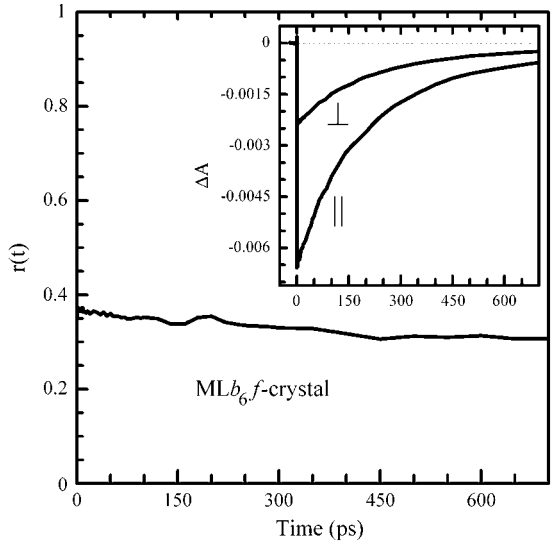

FIGURE 6 Time-resolved anisotropy of ΔA signal probed at 680 nm for the MLb_6f-crystal. (*Inset*) Corresponding anisotropic $\Delta A_{\parallel}$ and $\Delta A_{\perp}$ profiles.

Irreversible photodegradation of the monomeric Chl *a*

The level of Chl *a* photoprotection in the cytochrome b_6f complex was evaluated under aerobic conditions by monitoring irreversible photodegradation of Chl *a* in the MLb_6f complex and comparing it with the photodegradation kinetics of monomeric Chl *a* dissolved in ethanol, methanol, acetone, or Triton X-100 detergent. The photodegradation was assessed quantitatively by the integral of the Chl *a* Q_y absorbance band, which reflects the level of undamaged Chl *a* in the sample. Monomeric Chl *a* dissolved in organic solvents exhibited photodegradation kinetics similar to the kinetics previously observed (Jen and MacKinney, 1970a, 1970b). Fig. 7 *A* shows representative photodegradation kinetics of Chl *a* dissolved in ethanol. This profile can be fit with two exponential components, indicating that the degradation occurs with two characteristic lifetimes of 6 min and 2 h. The photodegradation kinetics of the Chl *a* in the MLb_6f complex also exhibits two exponential decay components (Fig. 7 *B*) but with much longer lifetimes of 14 h and 260 h. Thus, the Chl *a* in the MLb_6f complex is 130–140 times more stable than in solution.

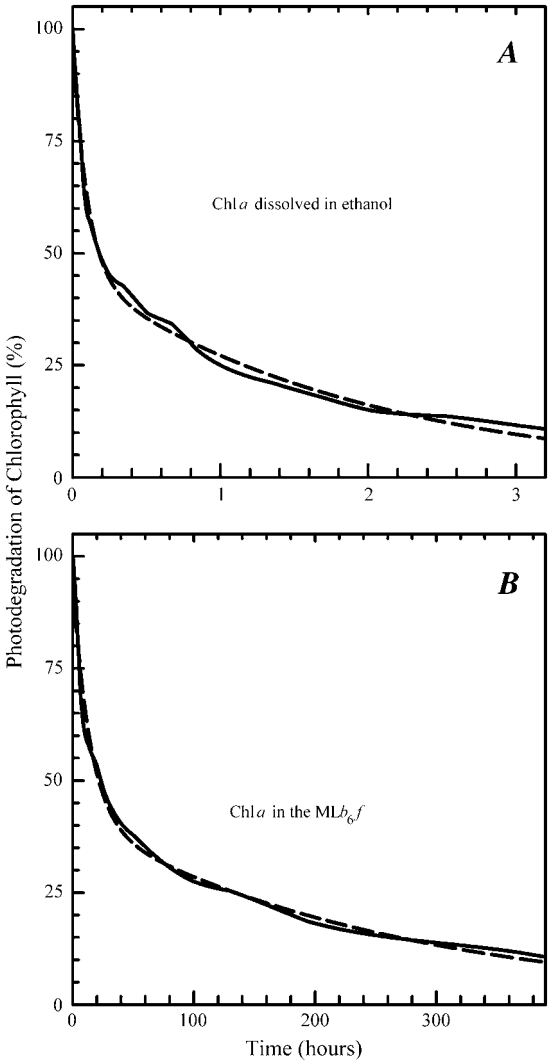

FIGURE 7 Irreversible degradation of Chl *a* dissolved in ethanol (*A*) and the Chl *a* in MLb_6f complex (*B*) as a function of irradiation time due to formation of singlet oxygen. Irradiation time is normalized to correspond to the same rate of excitation of Chl *a* as occurs under natural sunlight. The dashed curves represent the best fits to the data assuming a two-exponential decay.

DISCUSSION

Steady-state absorbance spectra reflect the Chl *a* local environment

The Chl *a* Q_y absorbance band for the b_6f complexes from spinach (Fig. 3, *inset*) and from *C. reinhardtii* (Pierre et al., 1997) are blue-shifted by ~3.5 nm with respect to the absorbance bands of the Chl *a* in SCb_6f and MLb_6f (Fig. 3, *inset*). This shift presumably arises from the variations in the local environment of the Chl *a*. According to the x-ray structures of the b_6f complexes (Kurisu et al., 2003; Stroebel et al., 2003), the surrounding nanospace of the Chl *a* is very similar in both ML and *C. reinhardtii* (the structure has not been yet determined for the b_6f complex from a higher plant). However, the mutual orientation and edge-to-edge distance between the Chl *a* and aromatic amino acid residues that are positioned in close proximity of the Chl *a* are distinctly different in the two cytochrome b_6f complexes—there are four Phe residues within 7 Å of the Chl *a* in the b_6f complexes from ML and only two in the complexes from *C. reinhardtii*. It has been shown by Ponamarev et al. (2000) that the difference in π-electrostatic interaction between heme and aromatic rings of Trp and Phe residues induced a spectral shift of the heme α absorption band in cytochrome *f* from a cyanobacterium relative to that in *C. reinhardtii*. We propose that the ~3.5 nm difference in the positions of the Chl *a* Q_y absorption bands may similarly stem from the different strength of π-electrostatic interaction between Phe and Chl *a* rings in these species. On the other hand, the observed spectral shift may be a cumulative effect of many small structural changes between the species, which cannot be resolved in the present x-ray structures. The noticeable broadening of the Chl *a* Q_y band in MLb_6f, if compared to MLb_6f-crystal, most probably arises from the presence of an inhomogeneous pool of nonspecifically bound Chl *a* molecules in the MLb_6f sample purified by conventional methods.

Unusually short lifetime of the Chl *a* singlet excited state

Peterman et al. (1998) reported that the singlet excited state of the Chl *a* in the functionally inactive monomeric cytochrome b_6f complex of *Synechocystis* PCC 6803 decays in 250 ± 20 ps, compared to the 5–6 ns lifetime reported for monomeric Chl *a* molecules in solution (Seely and Connolly,

1986). This was in good agreement with the measured low fluorescence quantum yield of the Chl *a* in the b_6f complex (1.8 ± 0.4%, Peterman et al., 1998) that was more than an order of magnitude lower than that of Chl *a* in methanol (~22%; Seely and Connolly, 1986). Our experiments confirmed that the unusually short Chl* lifetime is also characteristic of the enzymatically active dimeric b_6f complexes of ML and spinach, as well as inactive monomeric complexes from *Synechococcus* PCC 7002 suggesting, unexpectedly, that the local environment of the Chl *a* is similar in both active and inactive forms of the b_6f complex. In the following, we discuss three possible mechanisms that may cause the observed rapid quenching of the Chl *a* singlet excited state: i), increased rate of intersystem crossing, ii), interaction with the heme, and iii), excitation-induced electron transfer between the Chl *a* and nearby amino acid residue(s).

Increased rate of intersystem crossing

It is well documented that optically excited monomeric Chl *a* molecules in solution form a long-lived triplet excited state with ~64% yield as a result of intersystem crossing from the singlet excited state (Bowers and Porter, 1967; Seely and Connolly, 1986). Taking into account the measured excited state lifetime of 5–6 ns, the rate of intersystem crossing for Chl *a* in solvent is ~$(9\ \text{ns})^{-1}$. To account for the observed ~200 ps excited state lifetime of the Chl *a* in the b_6f complex, the local protein environment must increase the intersystem crossing rate 40–50-fold, which would result in Chl *a* triplet formation with 98% efficiency. Since the triplet excited state lifetime is ~200 ns (under aerobic conditions; Fujimori and Livingston, 1957), this will also significantly delay the recovery of the Chl *a* ground state. Our absorbance difference measurements, however, show that the recovery of the Chl *a* ground state in the b_6f complex occurs within ~200 ps and rules out the possibility that any significant amount of Chl *a* triplet state can be formed. Moreover, additional experiments performed using nanosecond absorbance spectrometry (not shown) revealed that the yield of Chl *a* triplet state formation in the b_6f complex is ≤2%, i.e., ≥30 times lower than that in solution. Thus, we can rule out intersystem crossing as a possible mechanism responsible for the unusually short singlet excited state lifetime of the Chl *a*.

Interaction with the nearby heme

According to the high-resolution crystal structure of the cytochrome b_6f complex (Kurisu et al., 2003; Stroebel et al., 2003), heme b_n of the cytochrome b_6 is parallel to the chlorin ring of the Chl *a*, from which it is separated by 16 Å (Fe-Mg center-to-center distance, Fig. 2). However, dithionite reduction of the initially oxidized low spin ferric heme revealed no dependence of the Chl* lifetime on the redox state of the nearby hemes, ruling out the involvement of the heme in the quenching process. Similar results were obtained by Peterman et al. (1998) for the enzymatically inactive b_6f complexes.

Excitation-induced electron transfer between the Chl a and nearby aromatic amino acid residues

It has been demonstrated by several groups (Karen et al., 1983; Mataga et al., 2000; Visser et al., 1987; Zhong and Zewail, 2001) that in flavin-binding proteins the electronic excited state of a chromophore can be efficiently quenched via electron transfer exchange with a nearby aromatic amino acid residue. The possible involvement of aromatic residues in fluorescence quenching of bacteriochlorophyll and chlorophyll molecules was also discussed by Li et al. (1997) and Peterman et al. (1998). The sequence of electron transfer events that may lead to quenching of the Chl *a* singlet excited state is depicted in the redox potential diagram shown in Fig. 8 *A*. When a Chl *a* molecule is excited, its electron donating (oxidation) potential (Chl/Chl^+) becomes more negative, whereas its electron accepting (reduction) potential (Chl/Chl^-) becomes more positive by a value approximately equal to the singlet excitation energy (Jones and Fox, 1994; Oda et al., 2001; Watanabe and Kobayashi, 1990). The energy of the Q_y transition of the Chl *a* is ~1.85 eV. Using the Chl/Chl^- of −0.88 V (Watanabe and Kobayashi, 1990), the electron accepting $\text{Chl}^*/\text{Chl}^-$ potential becomes anodic enough to initiate the first electron transfer step from the nearby Tyr residue since the Tyr/Tyr^+ electron donating potential is ~+0.93 V (DeFelippis et al., 1989; Harriman,

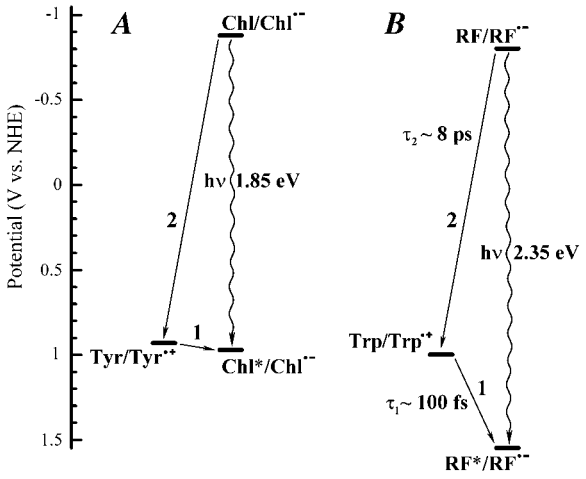

FIGURE 8 (*A*) Proposed quenching mechanism of the singlet excited state of the Chl *a* by the excitation-induced electron transfer process. Absorption of a photon promotes the Chl *a* into its singlet excited state and raises the oxidation potential from −0.88 V to +0.97 V (*wavy arrow*). In the following quenching process, the electron is first donated by a nearby Tyr to Chl*, transforming Chl* into unexcited Chl^- state (*arrow 1*). In the second electron transfer step (*arrow 2*), the Chl^- donates an electron to Tyr^+, resulting in neutral Chl and Tyr and completing the quenching process. (*B*) A similar scenario is proposed for fluorescence quenching of the RF in RF-binding protein with the experimentally measured lifetimes of electron transfer (Mataga et al., 2000; Zhong and Zewail, 2001).

1987; Jovanovic et al., 1991). Once an electron is transferred from the Tyr to the Chl*, the singlet excited state of the Chl *a* is transformed into a nonfluorescent reduced Chl^- state. The electron accepting Chl/Chl^- potential is, however, significantly more negative than the electron donating Tyr/Tyr^+ potential, forcing electron transfer from the reduced Chl^- back to the Tyr^+. As a result, both reactants return to their neutral ground states.

This model of the quenching kinetics of the Chl *a* singlet excited state can be described by the following sequential electron transfer scheme:

$$\boxed{Chl^{*}\ Tyr} \xrightarrow{k_1} \boxed{Chl^{\bullet-}\ Tyr^{\bullet+}} \xrightarrow{k_2} \boxed{Chl\ Tyr}, \qquad (2)$$

where k_1 and k_2 are the intrinsic rates of the respective electron transfer processes denoted by arrows ''1'' and ''2'' in Fig. 8. The time-resolved fluorescence measurements by Peterman et al. (1998) showed that the Chl *a* singlet excited state (Chl*) lifetime is ~250 ps (reflected in k_1 in the proposed scheme). However, the fluorescence measurements cannot detect the kinetics of the second electron transfer step (k_2) since both states involved in that step are nonfluorescent. In contrast, both electron transfer steps are reflected in the transient absorption difference kinetics reported in this study. To reproduce the essentially single-exponential ΔA kinetics measured at ~670 nm in the proposed scenario, the rate of the first electron transfer k_1 should be close to $(200\ ps)^{-1}$, whereas the rate of the second electron transfer step k_2 should be faster than $\sim(150\ ps)^{-1}$.

The mechanism of electron transfer and underlying theory have been described (see, for example, Gray and Winkler, 2003; Page et al., 2003). In the following, we used the Moser-Dutton semiempirical relationship (Page et al., 1999) to estimate the rates of exothermic (downhill) electron transfer, k_{ET}, for steps 1 and 2 (Fig. 8 *A*) at room temperature:

$$\log k_{ET} = 13 - 0.6(R - 3.6) - 3.1(\Delta G^{o} + \lambda)^2/\lambda, \qquad (3)$$

where R is the edge-to-edge distance between donor and acceptor, ΔG^{o} is the Gibbs free energy change for the electron transfer, and λ is the reorganization energy. By comparing the values of R and ΔG^{o} for all nearest aromatic residues, we inferred that Tyr-105 ($R = 6$ Å, Fig. 2) is the most likely residue responsible for electron-transfer mediated quenching of the Chl *a* excited state. This residue appears to be absolutely conserved among b_6f complexes isolated from different species. Using a value of $\lambda = 0.7$ eV for the reorganization energy (Page et al., 2003), Eq. 3 predicts a rate of $k_1 = (234\ ps)^{-1}$ for the first electron transfer step, which is in good agreement with the experimental value $(200\ ps)^{-1}$. However, this equation results in the rate constant $k_2 = (0.8\ \mu s)^{-1}$ for the second electron transfer, which is four orders of magnitude slower than the observed recovery rate of the Chl *a* ground state. This dramatic discrepancy may stem from uncertainties in reorganization energy and/or redox potential values. For example, using $\lambda = 1.05$ eV (still within the range of 0.9 ± 0.2 eV, cited by Page et al., 2003), Eq. 3 results in a rate of $(140\ ps)^{-1}$ for the second electron transfer, which is not inconsistent with the experimental results.

Similar high electron back-transfer rates to amino acid residues have been measured for the electron transfer mediated fluorescence quenching of the riboflavin (RF) in the RF-binding protein (Mataga et al., 2000; Zhong and Zewail, 2001). The RF/RF^- redox potential (−0.8 V, Fig. 8 *B*) is very close to that of the Chl/Chl^- (−0.88 V, Fig. 8 *A*), which makes the comparison between these two cases especially relevant. Using transient absorption and fluorescence spectroscopy, Zhong and Zewail (2001) determined that the first and second electron transfer steps occur with lifetimes ~100 fs and ~8 ps, respectively (Fig. 8 *B*), and proposed that electron-transfer exchange with the nearby Trp residue was responsible for the quenching of the RF excited state. The Trp/Trp^+ potential is 1.03 V (DeFelippis et al., 1989, 1991; Harriman, 1987), $R = 3.7$ Å and, using $\lambda = 0.7$ eV, Eq. 3 yields lifetimes 160 fs and 52 ns for the first and second electron transfer steps, respectively. As in the case of the Chl *a* and Tyr-105 in the cytochrome b_6f complex, the kinetics of the first electron transfer step in RF-binding protein is described very well by Eq. 3, but the rate calculated for the second electron transfer step is four orders of magnitude slower than the measured value. Agreement could, however, be attained if a reorganization energy $\lambda = 1.04$ eV is used for the second electron transfer step. This value of the reorganization energy is consistent with a value of $\lambda = 1.05$ eV for the $Chl^- \rightarrow Tyr^+$ electron transfer step required to reproduce the experimental data by the proposed kinetic model (Eq. 2). It was concluded that the electron transfer mediated quenching is the most plausible mechanism responsible for the unusually short lifetime of the singlet excited state of the Chl *a* in the cytochrome b_6f complex.

In principle, the kinetics of the intermediate Tyr^+ state could be monitored by its characteristic absorption difference signature at ~410 nm (Aubert et al., 1999). However, the corresponding extinction coefficient $\Delta\varepsilon \sim 3 \times 10^3\ M^{-1}cm^{-1}$ is small compared to the $\Delta\varepsilon \sim 6 \times 10^4\ M^{-1}cm^{-1}$ for the Chl *a* anion (Fujita et al., 1978), and it has not yet been possible to detect the Tyr^+ ion predicted to participate in this reaction. Alternatively, point mutations at the Tyr-105 site are expected to influence the lifetime of the Chl *a* in the proposed quenching scenario. Such studies are under way.

Photochemical degradation of the Chl *a* in the cytochrome b_6f complex and protection against singlet oxygen formation

Chl *a* is known for its ability to generate singlet oxygen (O_2*), which can chemically damage the Chl *a* itself as well as surrounding protein (Krinsky, 1979). Upon optical excitation, Chl *a* is promoted into its singlet excited state (Chl*), from where it can evolve into a long-lived triplet excited state (^{3}Chl*) through intersystem crossing. In the case of

monomeric Chl *a* in solution, the quantum yield of ^{3}Chl* formation could be as high as 64% (Bowers and Porter, 1967; Seely and Connolly, 1986). When Chl *a* in the triplet excited state encounters molecular oxygen, the electronic energy of the triplet excited state ^{3}Chl* is efficiently transferred to oxygen, resulting in an excited singlet oxygen O_2*.

In typical chlorophyll-containing proteins, the formation of singlet oxygen is prevented by positioning a Car close to a chlorophyll molecule, which effectively quenches the ^{3}Chl* through triplet-triplet energy transfer (Foote, 1976; Siefermann-Harms, 1987). However, triplet-triplet energy transfer from ^{3}Chl* to ^{3}Car* occurs through a Dexter-type exchange mechanism that is limited to short distances between these molecules (Renger, 1992; van Grondelle et al., 1994). Using the triplet-triplet energy transfer theory described in Dexter (1953) and data published elsewhere (Bodunov and Berberan-Santos, 2004; Schödel et al., 1998), it was estimated that triplet-triplet energy transfer from the ^{3}Chl* to ^{3}Car* in the cytochrome b_6f complex should occur in ~0.3 ms, which is much too slow to compete with singlet oxygen formation (≤10 ns, H. Kim et al., unpublished). Thus, the conventional mechanism of singlet oxygen protection by the direct triplet-triplet energy transfer process does not apply to the cytochrome b_6f complex.

Although the β-carotene is too far from the Chl *a* for direct protection, our photodegradation experiments (Fig. 7) demonstrate that the Chl *a* in the b_6f complex is 130–140 times more stable than in solution. We propose that protection, at least in part, is realized through specific arrangement of the local protein environment of the Chl *a* to ensure rapid quenching of the singlet excited state Chl*. Shortening of the Chl* lifetime from 5–6 ns to 200 ps causes a 25–30-fold decrease in the quantum yield of the ^{3}Chl* state formation and thus reduces the rate of O_2* formation. To the best of our knowledge, this mechanism of chlorophyll protection against singlet oxygen formation has not been yet reported.

In summary, the unusually short singlet excited state lifetime of the Chl *a* in the cytochrome b_6f complex can account only for 25–30-fold protection, whereas our experiments reveal that Chl *a* in the complex is 130–140 times more stable than monomeric Chl *a* molecule in solution. This implies that one or more additional unconventional protection mechanism(s) exist in the cytochrome b_6f complex.

This work was supported by grant 6903680 from the Purdue Research Foundation and the National Institutes of Health GM-38323. Some of the experiments were performed using Ames Laboratory equipment under the support of the Division of Chemical Sciences, Office of Basic Energy Sciences, and the U.S. Department of Energy. Ames Laboratory is operated by Iowa State University under Contract W-7405-Eng-82.

REFERENCES

Aubert, C., P. Mathis, A. P. M. Eker, and K. Brettel. 1999. Intraprotein electron transfer between tyrosine and tryptophan in DNA photolyase from *Anacystis nidulans*. *Proc. Natl. Acad. Sci. USA*. 96:5423–5427.

Bald, D., J. Kruip, E. J. Boekema, and M. Rögner. 1992. Structural investigations on cyt b_6f complex and PS I complex from the cyanobacterium *Synechocystis* PCC6803. *In* Photosynthesis: from Light to Biosphere, Part I. N. Murata, editor. Kluwer Academic Publishers, Dordrecht, The Netherlands. 629–633.

Berry, E. A., M. Guergova-Kuras, L.-S. Huang, and A. R. Crofts. 2000. Structure and function of cytochrome *bc* complexes. *Annu. Rev. Biochem.* 69:1005–1075.

Bodunov, E. N., and M. N. Berberan-Santos. 2004. Short-range order effect on resonance energy transfer in rigid solution. *Chem. Phys.* 301:9–14.

Bowers, P. G., and G. Porter. 1967. Quantum yields of triplet formation in solutions of chlorophyll. *Proc. R. Soc. A.* 296:435–441.

Cramer, W. A., G. M. Soriano, M. Ponamarev, D. Huang, H. Zhang, S. E. Martinez, and J. L. Smith. 1996. Some structural aspects and old controversies concerning the cytochrome b_6f complex of oxygenic photosynthesis. *Annu. Rev. Plant Physiol. Plant Mol. Biol.* 47:477–508.

Dawson, R. M. C., D. C. Elliot, W. H. Elliot, and K. M. Jones. 1986. Data for Biochemical Research. Clarendon Press, Oxford.

DeFelippis, M. R., C. P. Murthy, F. Broitman, D. Weinraub, M. Faraggi, and M. H. Klapper. 1991. Electrochemical properties of tyrosine phenoxy and tryptophan indolyl radicals in peptides and amino acid analogs. *J. Phys. Chem.* 95:3416–3419.

DeFelippis, M. R., C. P. Murthy, M. Faraggi, and M. H. Klapper. 1989. Pulse radiolytic measurement of redox potentials: the tyrosine and tryptophan radicals. *Biochemistry.* 28:4847–4853.

Dexter, D. L. 1953. A theory of sensitized luminescence in solids. *J. Chem. Phys.* 21:836–850.

Foote, C. S. 1976. Photosensitized oxidation and singlet oxidation: consequences in biological systems. *In* Free Radicals in Biology. W. A. Pryor, editor. Academic Press, New York. 85–133.

Fujimori, E., and R. Livingston. 1957. Interactions of chlorophyll in its triplet state with oxygen, carotene, etc. *Nature.* 180:1036–1038.

Fujita, I., M. S. Davis, and J. Fajer. 1978. Anion radicals of pheophytin and chlorophyll *a*: their role in the primary charge separations of plant photosynthesis. *J. Am. Chem. Soc.* 100:6280–6282.

Girvin, M. E., and W. A. Cramer. 1984. A redox study of the electron transport pathway responsible for generation of the slow electrochromic phase in chloroplasts. *Biochim. Biophys. Acta.* 767:29–38.

Gray, H. B., and J. R. Winkler. 2003. Electron tunneling through proteins. *Q. Rev. Biophys.* 36:341–372.

Hanson, L. K. 1990. Molecular orbital theory of monomer pigments. *In* Chlorophylls. H. Scheer, editor. CRC Press, Boca Raton, FL. 993–1014.

Harriman, A. 1987. Further comments on the redox potentials of tryptophan and tyrosine. *J. Phys. Chem.* 91:6102–6104.

Hoff, A. J., and J. Amesz. 1990. Visible absorption spectroscopy of chlorophylls. *In* Chlorophylls. H. Scheer, editor. CRC Press, Boca Raton, FL. 723–738.

Huang, D., R. M. Everly, R. H. Cheng, J. B. Heymann, H. Schagger, V. Sled, T. Ohnishi, T. S. Baker, and W. A. Cramer. 1994. Characterization of the chloroplast cytochrome b_6f complex as a structural and functional dimer. *Biochemistry.* 33:4401–4409.

Hunte, C., J. Koepke, C. Lange, T. Rossmanith, and H. Michel. 2000. Structure at 2.3 Å resolution of the cytochrome bc_1 complex from the yeast *Saccharomyces cerevisiae* co-crystallized with an antibody Fv fragment. *Struct. Fold. Des.* 8:669–684.

Iwata, S., J. W. Lee, K. Okada, J. K. Lee, M. Iwata, B. Rasmussen, T. A. Link, S. Ramaswamy, and B. K. Jap. 1998. Complete structure of the 11-subunit bovine mitochondrial cytochrome bc_1 complex. *Science.* 281: 64–71.

Jen, J. J., and G. MacKinney. 1970a. On the photodecomposition of chlorophyll *in vitro*—I. Reaction rates. *Photochem. Photobiol.* 11: 297–302.

Jen, J. J., and G. MacKinney. 1970b. On the photodecomposition of chlorophyll *in vitro*—II. Intermediates and breakdown products. *Photochem. Photobiol.* 11:303–308.

Joliot, P., and A. Joliot. 1994. Mechanism of electron transfer in the cytochrome *b/f* complex of algae: evidence for a semiquinone cycle. *Proc. Natl. Acad. Sci. USA.* 91:1034–1038.

Jones, W. E. Jr., and M. A. Fox. 1994. Determination of excited-state redox potentials by phase-modulated voltammetry. *J. Phys. Chem.* 98:5095–5099.

Jovanovic, S. V., S. Steenken, and M. G. Simic. 1991. Kinetics and energetics of one-electron-transfer reactions involving tryptophan neutral and cation radicals. *J. Phys. Chem.* 95:684–687.

Karen, A., N. Ikeda, F. Tanaka, and N. Mataga. 1983. Picosecond laser photolysis studies of fluorescence quenching mechanisms of flavin: a direct observation of indole-flavin singlet charge transfer state formation in solution and flavoenzymes. *Photochem. Photobiol.* 37:495–502.

Kramer, D. M., and A. R. Crofts. 1993. The concerted reduction of the high- and low-potential chains of the *bf* complex by plastoquinol. *Biochim. Biophys. Acta.* 1183:72–84.

Krinsky, N. I. 1979. Carotenoid protection against oxidation. *Pure Appl. Chem.* 51:649–660.

Kühlbrandt, W. 2003. Dual approach to a light problem. *Nature.* 426:399–400.

Kurisu, G., H. Zhang, J. L. Smith, and W. A. Cramer. 2003. Structure of the cytochrome b_6f complex of oxygenic photosynthesis: tuning the cavity. *Science.* 302:1009–1014.

Li, Y.-F., W. Zhou, R. E. Blankenship, and J. P. Allen. 1997. Crystal structure of the bacteriochlorophyll *a* protein from *Chlorobium tepidum*. *J. Mol. Biol.* 271:456–471.

Mataga, N., H. Chosrowjan, Y. Shibata, F. Tanaka, Y. Nishina, and K. Shiga. 2000. Dynamics and mechanisms of ultrafast fluorescence quenching reactions of flavin chromophores in protein nanonspace. *J. Phys. Chem. B.* 104:10667–10677.

Meinhardt, S. W., and A. R. Crofts. 1983. The role of cytochrome *b*-566 in the electron-transfer chain of *Rhodopseudomonas sphaeroides*. *Biochim. Biophys. Acta.* 723:219–230.

Metzger, S. U., W. A. Cramer, and J. Whitmarsh. 1997. Critical analysis of the extinction coefficient of chloroplast cytochrome *f*. *Biochim. Biophys. Acta.* 1319:233–241.

Moser, C. C., C. C. Page, R. Farid, and P. L. Dutton. 1995. Biological electron transfer. *J. Bioenerg. Biomembr.* 27:263–274.

Oda, N., K. Tsuji, and A. Ichimura. 2001. Voltammetric measurements of redox potentials of photo-excited species. *Anal. Sci.* 17:i375–i378.

Page, C. C., C. C. Moser, X. Chen, and P. L. Dutton. 1999. Natural engineering principles of electron tunnelling in biological oxidation-reduction. *Nature.* 402:47–52.

Page, C. C., C. C. Moser, and P. L. Dutton. 2003. Mechanism for electron transfer within and between proteins. *Curr. Opin. Chem. Biol.* 7:551–556.

Peterman, E. J. G., S. Wenk, T. Pullerits, L.-O. Pålsson, R. van Grondelle, J. P. Dekker, M. Rögner, and H. van Amerongen. 1998. Fluorescence and absorption spectroscopy of the weakly fluorescent chlorophyll a in cytochrome b_6f of *Synechocystis* PCC6803. *Biophys. J.* 75:389–398.

Pierre, Y., C. Breyton, D. Kramer, and J.-L. Popot. 1995. Purification and characterization of the cytochrome b_6f complex from *Chlamydomonas reinhardtii*. *J. Biol. Chem.* 270:29342–29349.

Pierre, Y., C. Breyton, Y. Lemoine, B. Robert, C. Vernotte, and J.-L. Popot. 1997. On the presence and role of a molecule of chlorophyll *a* in the cytochrome b_6f complex. *J. Biol. Chem.* 272:21901–21908.

Ponamarev, M. V., B. G. Schlarb, C. J. Howe, C. J. Carrell, J. L. Smith, D. S. Bendall, and W. A. Cramer. 2000. Tryptophan-heme π-electrostatic interactions in cytochrome *f* of oxygenic photosynthesis. *Biochemistry.* 39:5971–5976.

Renger, G. 1992. Energy transfer and trapping in photosystem II. *In* Topics in Photosynthesis, the Photosystems: Structure, Function and Molecular Biology. J. Barber, editor. Elsevier, Amsterdam, The Netherlands. 45–99.

Rich, P. 1984. Electron and proton transfers through quinones and cytochrome *bc* complexes. *Biochim. Biophys. Acta.* 768:53–79.

Savikhin, S., and W. S. Struve. 1994. Femtosecond pump-probe spectroscopy of bacteriochlorophyll *a* monomers in solution. *Biophys. J.* 67:2002–2007.

Savikhin, S., W. Xu, V. Soukoulis, P. R. Chitnis, and W. S. Struve. 1999. Ultrafast primary processes in photosystem I of the cyanobacterium *Synechocystis* sp. PCC 6803. *Biophys. J.* 76:3278–3288.

Schödel, R., K.-D. Irrgang, J. Voigt, and G. Renger. 1998. Rate of carotenoid triplet formation in solubilized light-harvesting complex II (LHCII) from spinach. *Biophys. J.* 75:3143–3153.

Seely, G. R., and J. S. Connolly. 1986. Fluorescence of photosynthetic pigments in vitro. *In* Light by Plants and Bacteria. J. Govindjee, J. Amesz, and D. C. Fork, editors. Academic Press, New York. 99–133.

Siefermann-Harms, D. 1987. The light-harvesting and protective functions of carotenoids in photosynthetic membranes. *Physiol. Plant.* 69:561–568.

Stroebel, D., Y. Choquet, J.-L. Popot, and D. Picot. 2003. An atypical haem in the cytochrome b_6f complex. *Nature.* 426:413–418.

Trumpower, B. L. 1990. The protonmotive Q cycle. Energy transduction by coupling of proton translocation to electron transfer by the cytochrome bc_1 complex. *J. Biol. Chem.* 265:11409–11412.

van Grondelle, R. J., J. P. Dekker, T. Gillbro, and V. Sundstrom. 1994. Energy trapping and transfer in photosynthesis. *Biochim. Biophys. Acta.* 1187:1–65.

Visser, A. J. W. G., A. van Hoek, T. Kulinski, and J. L. Gall. 1987. Time-resolved fluorescence studies of flavodoxin. Demonstration of picosecond fluorescence lifetimes of FMN in *Desulfovibrio* flavodoxins. *FEBS Lett.* 224:406–410.

Vladkova, R. 2000. Chlorophyll *a* self-assembly in polar solvent-water mixtures. *Photochem. Photobiol.* 71:71–83.

Watanabe, T., and M. Kobayashi. 1990. Electrochemistry of chlorophylls. *In* Chlorophylls. H. Scheer, editor. CRC Press, Boca Raton, FL. 287–315.

Xia, D., C.-A. Yu, H. Kim, J.-Z. Xia, A. M. Kachurin, L. Zhang, L. Yu, and J. Deisenhofer. 1997. Crystal structure of the cytochrome bc_1 complex from bovine heart mitochondria. *Science.* 277:60–66.

Zhang, H., and W. A. Cramer. 2004. Purification and crystallization of the cytochrome b_6f complex in oxygenic photosynthesis. *In* Photosynthesis Research Protocols. R. Carpentier, editor. Humana Press, Totowa, NJ. 67–78.

Zhang, H., D. Huang, and W. A. Cramer. 1999. Stoichiometrically bound β-carotene in the cytochrome b_6f complex of oxygenic photosynthesis protects against oxygen damage. *J. Biol. Chem.* 274:1581–1587.

Zhang, H., G. Kurisu, J. L. Smith, and W. A. Cramer. 2003. A defined protein-detergent-lipid complex for crystallization of integral membrane proteins: the cytochrome b_6f complex of oxygenic photosynthesis. *Proc. Natl. Acad. Sci. USA.* 100:5160–5163.

Zhang, Z., L. Huang, V. M. Shulmeister, Y.-I. Chi, K.-K. Kim, L.-W. Hung, A. R. Crofts, E. A. Berry, and S.-H. Kim. 1998. Electron transfer by domain movement in cytochrome bc_1. *Nature.* 392:677–684.

Zhong, D., and A. H. Zewail. 2001. Femtosecond dynamics of flavoproteins: charge separation and recombination in riboflavine (vitamin B_2)-binding protein and in glucose oxidase enzyme. *Proc. Natl. Acad. Sci. USA.* 98:11867–11872.